Ventrolateral medullary respiratory network and a model of cough motor pattern generation

ROGER SHANNON, DAVID M. BAEKEY, KENDALL F. MORRIS, AND BRUCE G. LINDSEY
Physiology and Biophysics and Neuroscience Program, College of Medicine, University of South Florida, Tampa, Florida 33612

Shannon, Roger, David M. Baekey, Kendall F. Morris, and Bruce G. Lindsey. Ventrolateral medullary respiratory network and a model of cough motor pattern generation. *J. Appl. Physiol.* 84(6): 2020–2035, 1998.—The primary hypothesis of this study was that the cough motor pattern is produced, at least in part, by the medullary respiratory neuronal network in response to inputs from "cough" and pulmonary stretch receptor relay neurons in the nucleus tractus solitarii. Computer simulations of a distributed network model with proposed connections from the nucleus tractus solitarii to ventrolateral medullary respiratory neurons produced coughlike inspiratory and expiratory motor patterns. Predicted responses of various "types" of neurons (I-DRIVER, I-AUG, I-DEC, E-AUG, and E-DEC) derived from the simulations were tested in vivo. Parallel and sequential responses of functionally characterized respiratory-modulated neurons were monitored during fictive cough in decerebrate, paralyzed, ventilated cats. Coughlike patterns in phrenic and lumbar nerves were elicited by mechanical stimulation of the intrathoracic trachea. Altered discharge patterns were measured in most types of respiratory neurons during fictive cough. The results supported many of the specific predictions of our cough generation model and suggested several revisions. The two main conclusions were as follows: *1*) The Bötzinger/rostral ventral respiratory group neurons implicated in the generation of the eupneic pattern of breathing also participate in the configuration of the cough motor pattern. *2*) This altered activity of Bötzinger/rostral ventral respiratory group neurons is transmitted to phrenic, intercostal, and abdominal motoneurons via the same bulbospinal neurons that provide descending drive during eupnea.

Bötzinger; ventral respiratory group; network simulations; computer modeling

THE ACT OF COUGHING is produced by complex concurrent and sequential changes in laryngeal and thoracoabdominal respiratory muscles. Cough is elicited by stimulation of receptors in the central airways. A cough usually begins with an enhanced inspiration due to contraction of the diaphragm and other inspiratory muscles acting in concert with the muscles that enlarge the upper airways (abductors). The next compressive phase is brief and is characterized by continued activity in the diaphragm and nearly simultaneous activation of the rib cage and abdominal expiratory muscles and upper airway muscles, which close the laryngeal folds (adductors). In the subsequent expulsive phase the diaphragm ceases activity and the glottis is opened as the adducting muscles relax and the abductors contract; the continued strong expiratory muscle activity results in high airflow velocities (for review see Refs. 25, 39, and 44).

Studies using pharmacological, electrical stimulation, and lesioning methods have identified the brain stem as the site of the cough motor pattern generator (for review see Refs. 25 and 44). The question left unanswered was whether the cough motor pattern is produced by the same brain stem neurons that generate the normal respiratory rhythm or by a separate "cough center." Engelhorn and Weller (15) and Jakus et al. (21, 22) reported that inspiratory- and expiratory-modulated neurons in the caudal lateral medulla and inspiratory neurons in the region of the nucleus tractus solitarii (NTS) increased firing rates during the appropriate phases of cough. These observations suggested the involvement of respiratory network neurons in cough.

Propriobulbar neurons in the rostral ventrolateral medulla have been implicated in respiratory rhythmogenesis and the formation of discharge patterns in respiratory premotoneurons and motoneurons (2, 3, 19, 40). Neurons in this region have been referred to as the rostral ventral respiratory group (rVRG) (3) and Bötzinger and pre-Bötzinger complexes (11, 19, 40). To be inclusive, this region of the respiratory network is referred to as the Bötzinger/rVRG (BÖT/rVRG) in this study. A recent report on some categories of neurons in this area of the brain stem has suggested roles for those neurons in cough (37). The intermediate and caudal regions of the ventral respiratory group (VRG) contain inspiratory and expiratory bulbospinal premotoneurons projecting to phrenic, intercostal, and abdominal motoneuron pools (33). The VRG also contains vagal and glossopharyngeal motoneurons that innervate upper airway muscles (3).

Cough is elicited by stimulation of airway rapidly adapting receptors and C fibers (39, 45). Pulmonary stretch receptor (PSR) afferents appear to play a significant but permissive role in the production of cough, probably by central facilitation of expiration (39, 45). The caudal NTS is the primary target of afferents from airway "cough" receptors (27). Rapidly adapting receptor second-order neurons in the NTS project to areas of the brain stem known to contain populations of neurons involved in respiratory control (17). Thus it appears that NTS neurons influenced by cough receptors may alter activity in the ventrolateral medulla respiratory network.

The present study addressed two major hypotheses: *1*) Bulbospinal drive to respiratory motoneurons during cough arises, at least in part, from the same medullary neurons involved in providing descending drive during normal breathing. *2*) The BÖT/rVRG neuronal network implicated in generating and shaping the eupneic pattern of breathing is also involved in producing the cough motor pattern. Specific hypotheses concerning responses of different BÖT/rVRG cell types

during cough were suggested by simulations of a network model (2) capable of generating respiratory patterns. The hypotheses were tested with in vivo experiments. The in vivo results were consistent with the main hypotheses and suggested several revisions in our model for cough generation.

Glossary

AUG	Augmenting, i.e., cells with peak firing rates during the second half of a phase
BÖT/rVRG	Bötzinger/rostral ventral respiratory group
BS	Bulbospinal, i.e., cells with axons projecting to the spinal cord
"Cough" receptors	Operationally defined rapidly adapting receptors and C-fiber afferents
CTH	Cycle-triggered histogram
DEC	Decrementing, i.e., cells with peak firing rates during the first half of a phase
E	Expiratory
E-AUG (BS)	Expiratory neuron with an augmenting discharge pattern; premotor excitatory bulbospinal
E-AUG (early)	BÖT/rVRG expiratory neuron with an augmenting discharge pattern; begins activity early in the phase and is active throughout
E-AUG (late)	BÖT/rVRG expiratory neuron with an augmenting discharge pattern; activity is limited primarily to the late part of the expiratory interval (stage 2 expiration)
E-DEC	Expiratory neuron with a decrementing firing rate; most active during the early-expiratory (postinspiratory) interval
EI	Neurons with activity traversing the expiratory-inspiratory transition
ELM	Expiratory laryngeal motoneuron
E-RECRUIT	Silent neuron that is evoked with an augmenting discharge pattern during the expiratory phase of cough; necessary addition to the model to produce a decrementing pattern in E-AUG (BS) neurons
EXP-MN	Spinal motoneuron to expiratory muscle
I	Inspiratory
i-cVRG	Intermediate-caudal ventral respiratory group
I-AUG (BS)	Inspiratory neuron with an augmenting firing rate during the phase (axon projects down spinal cord); does not exclude collateral axons in the brain stem
I-AUG (PB)	Inspiratory neuron with an augmenting firing rate during the phase (PB, propriobulbar; axon confined to brain stem)
I-DEC	Inspiratory neuron with a decrementing firing rate during the phase
I-DRIVER	Inspiratory neurons also active before the expiratory-inspiratory phase transition (I-EI) and with a relatively constant discharge rate throughout the inspiratory phase; definition specifically limited to BÖT/rVRG neurons with previously identified (2) excitatory functional links to other inspiratory neurons
IE	Neurons with activity traversing the inspiratory-expiratory phase transition
ILM	Inspiratory laryngeal motoneuron
LM	Laryngeal motoneuron
LUM1	Lumbar motor nerve
NRM	Non-respiratory-modulated, i.e., cells with no preferred phase of maximum firing rate
NTS	Nucleus tractus solitarii
P-ELM	Neurons inferred to be premotor to expiratory motoneurons
PHR MN	Phrenic motoneuron
P-ILM	Neurons inferred to be premotor to inspiratory motoneurons
PLAT	Plateau, i.e., cells with a relatively constant firing rate throughout a respiratory phase
P-LM	Neurons inferred to be premotor to laryngeal motoneurons
P-PHR	Neurons inferred to be premotor to phrenic motoneurons
PSR	Slowly adapting pulmonary stretch receptor
PUMP cell	Neuron excited by PSRs during lung inflation; no direct central respiratory drive
RECRUIT	Neurons active only during cough
RLN	Recurrent laryngeal nerve
STA	Spike-triggered average
?	Cells with low inspiratory or expiratory discharge rates that could not be further identified

METHODS

General Methods

Data were obtained from adult cats (2.5–4.1 kg) of either gender. Animals were initially anesthetized with intravenous thiopental sodium (28.0 mg/kg) and then decerebrated at the midcollicular level. Femoral arteries and veins were catheterized for monitoring of arterial blood pressure, acquisition of arterial blood samples, and administration of intravenous fluids and drugs. Arterial blood samples were analyzed periodically for P_{O_2}, P_{CO_2}, pH, and HCO_3^- concentration; these parameters were maintained within normal limits. Solutions of 5% dextrose in 0.45% NaCl, 5% dextran, or lactated Ringer solution were administered intravenously as needed to maintain a mean blood pressure of ≥100 mmHg. Before surgery was initiated, atropine (0.5 mg/kg im) was administered to reduce mucus secretion in the airways, and dexamethasone (5.0 mg im) was given to help prevent hypotension and minimize brain stem swelling. Animals were paralyzed by continuous intravenous infusion of gallamine triethiodide (4 $mg \cdot kg^{-1} \cdot h^{-1}$) and artificially ventilated through a tracheal cannula with a phrenic-driven respirator. End-tidal CO_2 was maintained at 4–5%. A bilateral thoracotomy was performed to minimize brain stem movement. When necessary, the fraction of inspired O_2 was increased to prevent hypoxemia, which often occurs during long-term experiments because of ventilation-perfusion mismatching resulting from the open

chest. The functional residual capacity of the lungs in thoracotomized animals was maintained within a normal range by adjustment of end-expiratory pressure. Rectal temperature was maintained at 38 ± 0.5°C by a servo-controlled heating pad. The animals were placed prone in a stereotaxic frame.

Nerve Recordings

The right cranial iliohypogastric (L_1) and left phrenic (C_5) nerves were desheathed and cut, and their efferent activity was recorded with bipolar silver electrodes in pools of mineral oil. The right recurrent laryngeal nerve was desheathed and cut close to the larynx to leave the tracheal innervation intact; efferent activity was recorded with bipolar silver electrodes covered with cotton pledgets saturated with mineral oil. Nerve signals were amplified and filtered (band pass 0.1–5 kHz). Phrenic and lumbar nerve discharges were integrated with a leaky resistance-capacitance circuit (0.2-s time constant) and recorded on a polygraph to monitor the effectiveness of the stimuli to elicit cough.

Neuron Recordings and Characterization

An occipital craniotomy was performed, and portions of the caudal cerebellum were removed by suction to expose the medulla. Neurons in the BÖT/rVRG and i-cVRG were monitored simultaneously with two independently controlled planar arrays of tungsten microelectrodes (10–12 MΩ). In the initial experiments, individual electrodes in an array were fixed to each other. Each array consisted of six to eight microelectrodes with adjacent tips 150–200 μm apart. These interelectrode distances permitted the recording of separate single neurons on adjacent electrodes. In later experiments the depth of each electrode was adjusted individually with micromotor controllers developed by us. Signals were amplified and filtered (band pass 0.1–5 kHz). The medullary surface was covered by a pool of warm mineral oil.

Regions of the ventrolateral medulla that were searched for respiratory neurons included those reported by numerous authors (3, 16, 40), as well as by us (29, 41), to contain the respiratory network of interest (BÖT/rVRG: 3.0–5.5 mm rostral to obex, 3.0–4.5 mm lateral to midline, 3.0–5.5 mm below dorsal surface; i-cVRG: 2.0 mm rostral to 4.0 mm caudal to obex, 3.0–5.0 mm lateral to midline, 2.5–4.5 mm below dorsal surface). Neurons antidromically activated (positive collision test) from the spinal cord were designated bulbospinal. Bipolar stainless steel electrodes were placed in the ventral spinal cord at the T_1 level contralateral to medullary recording sites. Single pulses ranging in intensity from 1 to 10 V and 0.1-ms duration were used. Spike-triggered averaging of contralateral phrenic and ipsilateral recurrent laryngeal nerve efferent activities was used to identify phrenic premotoneurons and laryngeal motoneurons and other neurons that functionally influenced them (see *Spike-Triggered Averaging of Efferent Nerve Signals*).

Evoking Fictive Cough

Mechanical stimulation of the intrathoracic trachea has been used in spontaneously breathing animals to elicit cough and in paralyzed, ventilated animals to produce coughlike patterns (fictive cough) in respiratory motor activity (5, 25, 44). Fictive coughing was elicited by rubbing sections of the intrathoracic trachea (midcervical to carinal region) with two loops of polyethylene tubing attached to a thin wire inserted through a port in the tracheal cannula. The loops of tubing were configured as ellipsoids (1 cm diameter). Multiple coughs were usually elicited with minimal stimulation of the trachea. When more than one cough occurred in a trial, only the first one was analyzed. Cough was characterized by a large increase in phrenic activity coincident with or immediately followed by a large increase in lumbar activity. Between stimulus trials the polyethylene tubing was retracted into the tracheal cannula to prevent stimulation of the trachea. At least five separate episodes of cough were produced. Each stimulus trial was separated by ≥1 min, which was sufficient for inspiratory and expiratory burst patterns to return to control. Because PSR feedback to the medulla is important in the production of cough (39, 45), a phrenic-driven ventilator was used to allow matching of PSR activity with central inspiratory activity (5).

Data Acquisition

Signals from the microelectrode arrays, efferent nerve activities, arterial blood pressure, tracheal pressure, and stimulus information were recorded on magnetic tape for off-line analysis. During the experiments, appropriate signals were monitored on oscilloscopes, a polygraph, and audio monitors.

Data Entry and Preprocessing

Multifiber efferent phrenic, lumbar, and recurrent laryngeal nerve activities were integrated (full-wave-rectified signal to a resistor-capacitor integrator; time constant 0.2 s) to obtain a moving time average of activity in the nerves. These analog signals, together with arterial blood pressure, tracheal pressure, stimulus timing signals, and signals from each microelectrode, were entered into a computer via a 16-channel analog-to-digital converter. Because the signals from a single experimental run were recorded on two 16-channel FM instrument recorders, a synchronization timing pulse recorded on each tape was also entered to permit later merging of data from the tapes into one master file (34). During the merge, time stamps were derived from the integrated phrenic signal to indicate the onset of each inspiratory and expiratory phase (26). Action potentials of single neurons were converted to times of occurrence with spike-sorting software (Datawave Technology). These data files were transferred to a Hewlett-Packard 9000/735 computer for subsequent processing and analysis. The signals of efferent multiunit nerve activities and the common synchronization timing pulses were also digitized (5 kHz) with a 16-bit ADC488/16 analog-to-digital converter hosted by a Hewlett-Packard 9000/380 computer. These files were subsequently analyzed with the corresponding spike files for spike-triggered averaging, as described below. The program Xscope (28) provided a graphical representation of the times of action potentials and other digital and analog signals. The program allowed additional event codes to be added and graphically confirmed the selection of data segments to be written as separate files for later analysis.

Spike Train Analysis Methods for Each Single Neuron

Spike trains were subjected to two statistical evaluations of respiratory modulation, and a measure of respiratory modulation, η^2, was calculated (34, 38). Neuron cycle-triggered histograms were compared with phrenic cycle-triggered histograms to define the respiratory phase (inspiratory or expiratory) in which the neuron was most active. An autocorrelogram was computed for each spike train to ensure that each train of events represented the activity of one unit. Spike trains were also evaluated statistically for changes in discharge pattern during cough. The peak firing rate, average firing rate, onset of firing, and duration of firing of the neuron during the first cough cycle, averaged over five trials, had to

be significantly different from the mean for five control cycles just preceding the cough ($P < 0.05$, Student's *t*-test).

Spike-Triggered Averaging of Efferent Nerve Signals

Unrectified and full-wave-rectified signals from phrenic and recurrent laryngeal nerves were averaged using the spikes of each simultaneously recorded neuron as trigger events. Nerve signals were high-pass filtered (40 Hz, 3-dB cutoff) and sampled at 5 kHz with 16-bit accuracy. Short-latency, short-duration offset peaks (1.5 ± 0.3 ms, <1.1-ms half-width) in rectified phrenic nerve averages were used as evidence that the cell was either *1*) a premotoneuron that projects to the monitored motoneuron pool or *2*) tightly synchronized with such a cell by functionally antecedent shared inputs (8, 24). A short-latency (1.5–3.5 ms) (9), short-duration feature in the unrectified and rectified recurrent laryngeal nerve average provided evidence that the recorded neuron was a laryngeal motoneuron (7). Presence of the feature in the rectified but not the unrectified signal suggested that the neuron was characterized was either 1 or *2*.

Network Simulations

Detailed hypotheses were derived from neural network simulations performed with SYSTM11 (31). Functional connections for NTS cough and PSR relay neurons (pump) and additional populations of VRG neurons were added to a previously described model (2). At each integration step (0.5 ms of simulated time) the following state variables were updated: membrane potential (E_{ij}), threshold for action potential (Th_{ij}), post-action potential potassium conductance [$G_{K(ij)}$], and synaptic input currents (G_{ijk}) for each neuron (j) of each population (i) and each synaptic type (k). If the membrane potential of any cell, calculated according to a standard equivalent circuit model, exceeded threshold, an action potential was recorded in that cell, the potassium conductance was activated, and the targets of the cell received a synaptic input current. Terminals from each population of neurons were randomly distributed on each specified target population. Connections between individual neurons were made according to a sequence of pseudorandom numbers calculated from a unique seed number for each source-to-target connection. Networks were simulated on a Hewlett-Packard 9000/735 computer. Program output was displayed and analyzed with the same methods described above for biological network analysis.

RESULTS

Simulated Cough Model

Figure 1*A* shows a scheme of BÖT/rVRG and i-cVRG network connections (large box enclosed in dashed line) inferred primarily from spike train analysis and spike-triggered averaging of synaptic potentials (for review see Refs. 3, 14, 16, and 35 and Refs. 1, 2, 13, 28–30, 34, and 41). A network of relatively simple neurons with varying degrees of accommodation, but no endogenous bursting properties, was simulated to determine whether the inferred connections were plausible and sufficient to generate cough motor discharge patterns similar to those observed in vivo. This network included the functional connections and most of the neurons currently proposed to have a role in respiratory rhythm generation. The core of this scheme (shaded areas in Fig. 1) was a previously described model that generates a eupneic respiratory rhythm (2). Initial "baseline" parameters for the subset of the network described previously were derived from that work. As additional populations were added, values of small subsets of parameters were varied. The parameters were adjusted to achieve a closer match to the physiological measures, and the process was repeated.

New additions to the simulated network (2) included bulbospinal inspiratory and expiratory premotoneurons [I-AUG (BS) and E-AUG (BS)], recruited expiratory neurons, and hypothesized effects of cough receptor and PSR inputs. The working hypothesis was that those neurons in the respiratory network implicated in the control of eupneic respiratory phase timing and motor pattern generation are also involved in configuring the cough motor pattern. The connections from NTS PUMP cells and second-order cough neurons to model neurons were hypothesized to be influences that, through their joint action, produce a cough motor pattern (39, 44).

Table 1 lists the values for parameters used to define each population of neurons. All populations except E-DEC contained 300 neurons. Ninety-nine E-DEC neurons were simulated, because cells with this particular discharge pattern were encountered less often in previous work than those with I-AUG, I-DEC, and E-AUG discharge patterns (29, 41). The membrane potentials of neurons were influenced by steady inward currents and random excitatory and inhibitory inputs from "fibers" originating outside the network, as enumerated in Table 2. The effects of connections among the simulated neurons were superimposed on these unpatterned baseline influences. Cough receptors were represented by a fiber population ($n = 300$); each fiber had a firing probability of 0.05 at each time step when activated. Outputs from the population representing phrenic motoneurons were used to generate inspiratory-modulated PUMP cell activity.

Three types of synapses were used in all simulations: type 1 excitatory (equilibrium potential of 115.0 mV above resting membrane potential, time constant 1.5 ms), type 1 inhibitory (equilibrium potential −25.0 mV below resting membrane potential, time constant 1.5 ms), and type 2 inhibitory (equilibrium potential −25.0 mV below resting membrane potential, time constant 2.0 ms). The efficacy of connections between populations of neurons was also defined by the change in conductance (synaptic strength variable) associated with each action potential at a synapse and the number of terminals for each axon. Table 2 shows these values, synaptic type, and the conduction time parameter for all sets of connections. The connectivity matrix (Table 3) shows the number of neurons in each target population innervated by each source neuron in each population. Corresponding values are also shown for source neurons that innervated each target neuron in each population. These data indicate the extent of divergence and convergence. Most neurons in each source population made a single terminal connection with each target neuron.

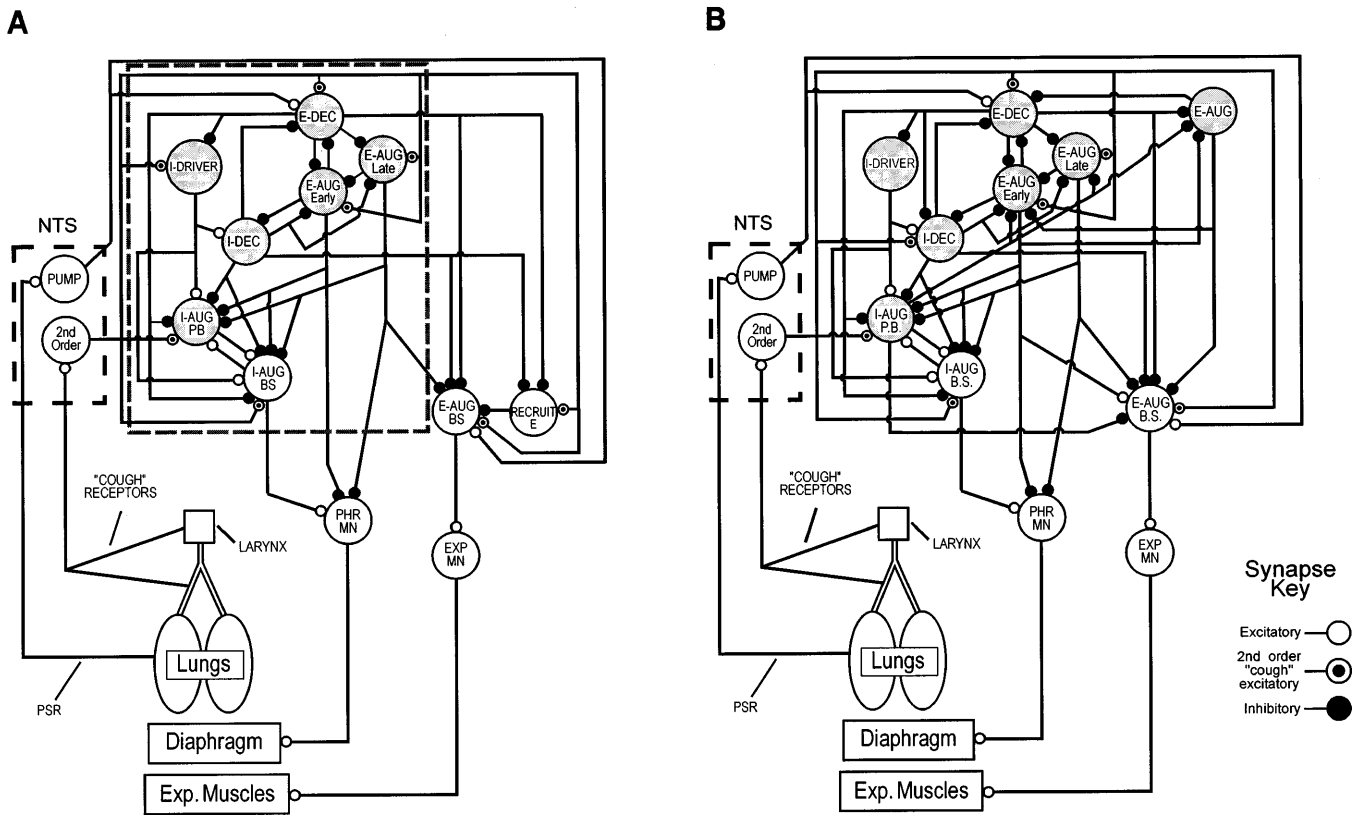

Fig. 1. Original (*A*) and revised (*B*) cough network models: scheme of BÖT/rVRG network connections and inputs from NTS cough receptor 2nd-order neurons and PSR PUMP cells. Exp, expiratory. See *Glossary* for definition of other abbreviations.

The cough model incorporated three major hypotheses. *1*) Airway cough receptors activate neurons in the NTS that distribute information concurrently to different neuron populations in the BÖT/rVRG and i-cVRG. *2*) A network composed of BÖT/rVRG neurons produces the cough motor pattern. *3*) Bulbospinal drive to respiratory motoneurons during cough arises, at least in part, from the same medullary neurons that provide drive during eupneic breathing. The model network generated a simulated cough motor pattern during stimulation of the cough afferents (PHR and LUM1 in Fig. 2). Each neuron trace in Fig. 2 is the integrated spike activity from a representative neuron in each indicated population generated during simulated eupneic respiratory cycles and subsequent coughs. We emphasize that we have conducted only a limited exploration of the simulation parameter space. The simulations included ILM and ELM responses during cough. The laryngeal motoneurons and specific neuron connections controlling their responses are not in-

Table 1. *Parameter values for representative network*

Population	No. of Neurons in Population (N)	Resting Threshold, mV (THO)	Membrane τ, ms (TMEM)	Postspike Increase in G_K^+ (B)	Postspike $G_K^+ \tau$, ms (TGK)	Adaptation Threshold Increase (C)	Adaptation τ, ms (TTH)
I-DRIVER	300	10.0	7.0	25.0	5.0	0.18	500.0
I-DEC	300	10.0	5.0	25.0	3.3	0.55	500.0
I-AUG (PB)	300	10.0	6.0	25.0	3.8	0.08	500.0
I-AUG (BS)	300	10.0	6.0	25.0	3.8	0.08	500.0
E-DEC	99	10.0	9.0	27.0	2.5	0.85	500.0
E-AUG (early)	300	10.0	6.0	27.0	2.5	0.04	500.0
E-AUG (late)	300	10.0	9.0	27.0	2.5	0.10	500.0
E-RECRUIT	300	10.0	9.0	27.0	2.5	0.10	500.0
E-AUG (BS)	300	10.0	9.0	27.0	2.5	0.3	500.0
PUMP cell	300	10.0	6.0	25.0	3.8	0.08	500.0
PHR MN	300	10.0	6.0	25.0	3.8	0.08	500.0

Variable names used by MacGregor (31) are in parentheses. N, number of neurons simulated in each population; THO, resting threshold of neurons; TMEM, membrane time constant; B, amplitude of postspike increase in K^+ conductance; TGK, time constant of K^+ conductance decay after an action potential; C and TTH, change in threshold associated with spike adaptation. C is amount of threshold increase for a particular membrane potential; its value is between 0 and 1. TTH is time constant of rise in threshold with spike adaptation. See *Glossary* for definition of other abbreviations.

Table 2. *Extrinsic "fiber" and current inputs for representative network*

Target	Source			
	Excitatory population	Inhibitory population	"Cough receptor" input	Current
I-DRIVER				8.0
nt	48	48	48	
st	ex-1	in-1	ex-1	
ss	0.02	.01	0.0075	
I-DEC				7.0
nt	16	16		
st	ex-1	in-1		
ss	0.0025	0.02		
I-AUG (PB)				12.0
nt			48	
st			ex-1	
ss			0.005	
I-AUG (BS)				12.0
nt	24			
st	ex-1			
ss	0.02			
E-DEC				15.0
nt	16	16	48	
st	ex-1	in-1	ex-1	
ss	0.02	0.02	0.005	
E-AUG (early)				17.0
nt	48	48	48	
st	ex-1	in-1	ex-1	
ss	0.025	0.07	0.0025	
E-AUG (late)				17.0
nt	48	48	48	
st	ex-1	in-1	ex-1	
ss	0.03	0.08	0.0025	
E-RECRUIT				
nt			75	
st			ex-1	
ss			0.055	
E-AUG (BS)				17.0
nt	48	48	75	
st	ex-1	in-1	ex-1	
ss	0.03	0.08	0.025	
PUMP cell				
nt	42			
st	ex-1			
ss	0.03			

Each fiber population had 300 elements. Each fiber had a 0.05 probability of firing at each time step in simulation. nt, Number of terminals/axon; st, synaptic type; ss, synaptic strength; in, inhibitory; ex, excitatory. Conduction time parameter was 1 ms for all fiber populations. See *Glossary* for definition of other abbreviations.

cluded in Fig. 1*A* or related tables, because mechanisms configuring laryngeal motoneurons are not included in this in vivo study. This study focused on the neurons controlling the respiratory thoracoabdominal motoneurons. The ELM responses in particular were included in Fig. 2 to approximate the compressive period. The results of the simulations (Fig. 2) suggested a coherent set of physiologically plausible hypotheses for the responses of neurons controlling the inspiratory and expiratory pump muscles. Specific hypotheses on neuron responses and interactions during cough are summarized below for each of three phases of cough. To place the hypotheses in context, the compressive phase and ILM and ELM activities are included.

Inspiratory phase of cough. Initially, all propriobulbar (I-DRIVER, I-AUG PB, and I-DEC) and premotor bulbospinal inspiratory [I-AUG (BS)] neurons are excited (directly or indirectly) by NTS cough afferent second-order neurons, which leads to an increased ramp and duration of inspiratory motor (PHR) activity. ILMs also increase activity during this phase. Expiratory neurons are suppressed, at least during early inspiration; they are inhibited by I-DEC neurons. The inspiratory phase is terminated by the inhibitory actions of propriobulbar E-DEC and early E-AUG cells. The increased E-DEC and E-AUG neuron activity is due to a decrease in I-DEC inhibition, and excitation is caused by increased PSR (via PUMP cells) and cough receptor activity.

Compressive phase of cough. A large increase in activity of bulbospinal premotor expiratory neurons [E-AUG (BS)] and ELMs occurs near the end of the inspiratory phase. E-AUG (BS) cells increase activity primarily because of excitation by cough receptors and PSRs. Other factors that promote this expiratory activity include disinhibition by I-DEC neurons and postinhibitory rebound. At the end of the compressive phase, ELM activity ceases.

Expulsive phase of cough. For a short period after the compressive phase, activity of E-AUG (BS) neurons, and thus expiratory motoneurons (EXP MN), continues to increase. As the expiratory phase progresses, bulbospinal E-AUG neurons, and thus expiratory motoneurons (LUM1), and muscles now have a decrementing discharge pattern. This pattern is shaped by the inhibitory actions of propriobulbar E-AUG late neurons with activity that begins after the onset of the expiratory phase, E-recruit neurons, early-onset I-DEC and I-AUG activity, and decreasing PSR activity. ILM activity is again elevated during this phase.

In Vivo Studies

Phrenic and lumbar nerve pattern changes during fictive cough. Mechanical stimulation of the intrathoracic trachea elicited alterations in phrenic and lumbar motor nerve discharge patterns that were qualitatively similar to those reported previously in unanesthetized or anesthetized spontaneously breathing animals and anesthetized or decerebrate paralyzed animals (5, 25, 44). Fictive coughs consisted generally of a large increase in phrenic and then lumbar activities; the increase in lumbar activity occurred just before, coincident with, or immediately after the termination of peak phrenic activity (Figs. 3–5). The duration of phrenic discharge was always increased over control. The expiratory duration was usually greater than control when a single cough was provoked (Fig. 5), whereas a shorter expiratory duration usually accompanied multiple coughs (Fig. 3*B*).

Neuron recordings from BÖT/rVRG and i-cVRG. The data are from 306 neurons recorded during 51-cough series in 24 cats. Table 4 presents neuron discharge patterns, axonal projections, and changes in peak firing rate during cough. All neurons did not undergo bulbospinal or spike-triggered average tests. Many of the neurons that were tested had negative bulbospinal, recurrent laryngeal motoneuron, or premo-

Table 3. *Connectivity matrix for simulated network*

	Target										
Source	I-EI	I-DEC	I-AUG (PB)	I-AUG (BS)	E-DEC	E-AUG-e	E-AUG-I	E-REC	E-AUG-(BS)	PUMP	PHR
I-DRIVER											
nt		50	50	45							
st		ex-1	ex-1	ex-1							
ss		0.027	0.015	0.035							
dv		46.1	46.1	41.9							
cn		46.1	46.1	41.9							
I-DEC											
nt			50	50	20	50	50	50	60	50	
st			in-2	in-2	in-2	in-2	in-2	in-2	in-2	in-2	
ss			0.09	0.09	0.16	0.18	0.18	0.3	0.25	0.18	
dv			46.1	45.9	18.2	46.0	46.0	46.1	54.3	39.4	
cn			46.1	45.9	55.1	46.0	46.0	46.1	54.3	118.1	
I-AUG (PB)											
nt				25							
st				ex-1							
ss				0.02							
dv				24.1							
cn				24.1							
I-AUG (BS)											
nt			25								50
st			ex-1								ex-1
ss			0.02								0.045
dv			24.0								46.1
cn			24.0								46.1
E-DEC											
nt	60		50	50		50	50	85	50		
st	in-2		in-1	in-1		in-1	in-1	in-1	in-1		
ss	1.4		0.1	0.1		0.18	0.3	0.45	0.3		
dv	54.6		46.1	46.1		46.3	46.3	74.3	46.3		
cn	18.0		15.2	15.2		15.3	15.3	24.5	15.3		
E-AUG-e											
nt		50	100	100	25						65
st		in-2	in-1	in-1	in-1						in-1
ss		0.55	0.03	0.05	0.008						0.004
dv		46.1	85.2	85.2	22.3						58.5
cn		46.1	85.2	85.2	67.5						58.5
E-AUG-I											
nt			100	100	25	50			50	100	100
st			in-1	in-1	in-1	in-1			in-1	in-1	in-1
ss			0.075	0.135	0.016	0.07			0.05	0.15	0.08
dv			85.2	85.1	22.3	46.3			46.3	63.5	85.1
cn			85.2	85.1	64.5	46.3			46.3	190.4	85.1
E-REC											
nt									75	50	
st									in-1	in-1	
ss									0.065	0.15	
dv									66.5	39.6	
cn									66.5	118.7	
PUMP											
nt					48				48	48	
st					ex-1				ex-1	ex-1	
ss					0.01				0.01	0.01	
dv					38.2				44.4	38.2	
cn					115.8				44.4	114.6	

dv, Mean number of target neurons innervated by each source neuron in each population; maximum standard deviation for a divergent set of projections was 15% of mean. cn, Mean number of source neurons that innervated each target neuron in each population; maximum standard deviation for a convergent set of projections was 25% of mean. See *Glossary* and Table 2 footnote for definition of other abbreviations.

toneuron tests. These latter unidentified respiratory-modulated cells may be propriobulbar neurons involved in the control of breathing, cranial motoneurons innervating muscles of the upper airways, other than laryngeal, and smooth muscle of the lower airways (3), and/or autonomic neurons involved in the regulation of cardiovascular function (18, 32). Despite these uncertainties, responses during cough allowed the separation of neurons with similar control discharge patterns into subpopulations with different putative functions. Neuron responses during in vivo cough are presented below in an order that first allows comparison with neurons included in the network model (Figs. 1*A* and 2). Figure 4 illustrates the activity of simultaneously recorded neurons. The number of neurons recorded simultaneously in each data set ranged from 1 to 17

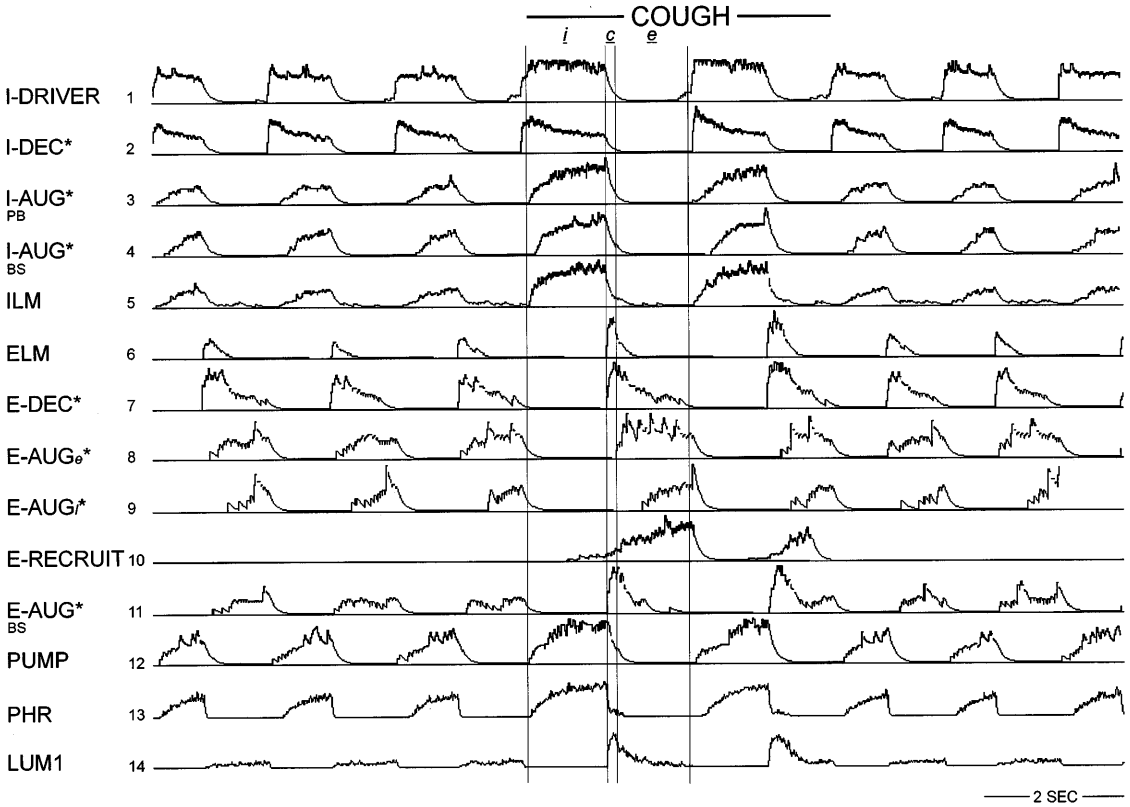

Fig. 2. Computer-simulated cough motor pattern. Neuron, phrenic, and lumbar nerve discharge rates are displayed as moving time averages (100-ms time constant). *Model predictions confirmed by in vivo results from this study. i, c, and e, Inspiratory, compressive, and expulsive phase of cough, respectively.

(mean 6). Such data document concurrent and sequential changes in activity during cough under identical conditions.

I-PLAT NEURONS WITH PUTATIVE ROLES AS I-DRIVER NEURONS (BÖT/ROSTRAL VRG). Five neurons had plateau (PLAT) discharge patterns similar to those proposed to provide excitatory drive to other medullary inspiratory neurons (2, 16, 34, 41) (Fig. 3). They had negative bulbospinal and laryngeal motoneuron tests. They responded during in vivo cough with a prolonged duration of activity. Four of these cells showed no change in peak activity (Fig. 3*A*, *trace 2*), and one had an increase in peak activity in the latter part of the inspiratory phase (Fig. 3*B*). Spike-triggered averaging suggested that this latter cell was functionally premotor to ILMs and phrenic motoneurons (STAs in Fig. 3*C*). The STA features were interpreted as direct and synchronous actions of the reference cell on the targets (scheme in Fig. 3*E*). Four of these putative I-DRIVER neurons did not respond during cough as proposed in the model (Fig. 2, *trace 1*); i.e., peak activity did not increase. One other I-PLAT cell was identified as an ILM. The I-AUG cell in Fig. 3*A* (*trace 1*) is shown to illustrate the use of spike-triggered averaging to identify laryngeal motoneurons vs. functional premotoneurons. The short-latency, sharp peak features in the rectified and unrectified STA in Fig. 3*D* are consistent with this unit being an ILM.

I-DEC NEURONS (BÖT/ROSTRAL VRG). Twenty-two neurons showed peak firing rates in the first half of the inspiratory phase (I-DEC). They exhibited diverse discharge patterns during control periods and especially during in vivo cough. Eight I-DEC cells (1 BS, 0 P-PHR, 0 P-LM, 0 LM, 1 not tested) responded during cough with increased early peak activity and an extended DEC pattern (Fig. 4, *trace 1*). The responses of the six putative propriobulbar neurons were consistent with the model simulation (Fig. 2, *trace 2*). Nine other I-DEC neurons (0 BS, 0 P-PHR, 1 P-LM, 0 LM, 4 not tested) discharged throughout most of the inspiratory phase during control and then showed a predominantly AUG pattern during cough (Fig. 5, *trace 3*). Four additional I-DEC neurons (0 BS, 0 P-PHR, 1 P-LM, 0 LM) that discharged briefly at the onset of the inspiratory phase had no change in peak discharge pattern during cough but did show a prolonged firing time.

I-AUG (PB) AND I-AUG (BS) NEURONS (INTERMEDIATE-CAUDAL AND BÖT/ROSTRAL VRG). During in vivo cough, all I-AUG cells (34 i-cVRG, 22 BÖT/rVRG) increased activity in a manner similar to the enhanced AUG pattern of the phrenic nerve (Fig. 4, *trace 6*). These responses agree with the model simulation (Fig. 2, *traces 3* and *4*). Four I-AUG neurons (2 i-cVRG and 2 BÖT/rVRG) were characterized with spike-triggered averaging tests as being premotor to ILM. Twenty-one i-cVRG and three BÖT/rVRG I-AUG neurons were characterized as bulbospinal. Two BÖT/rVRG cells were laryngeal motoneurons.

E-DEC NEURONS (BÖT/ROSTRAL VRG). Seven E-DEC neurons increased peak activity near the inspiratory-

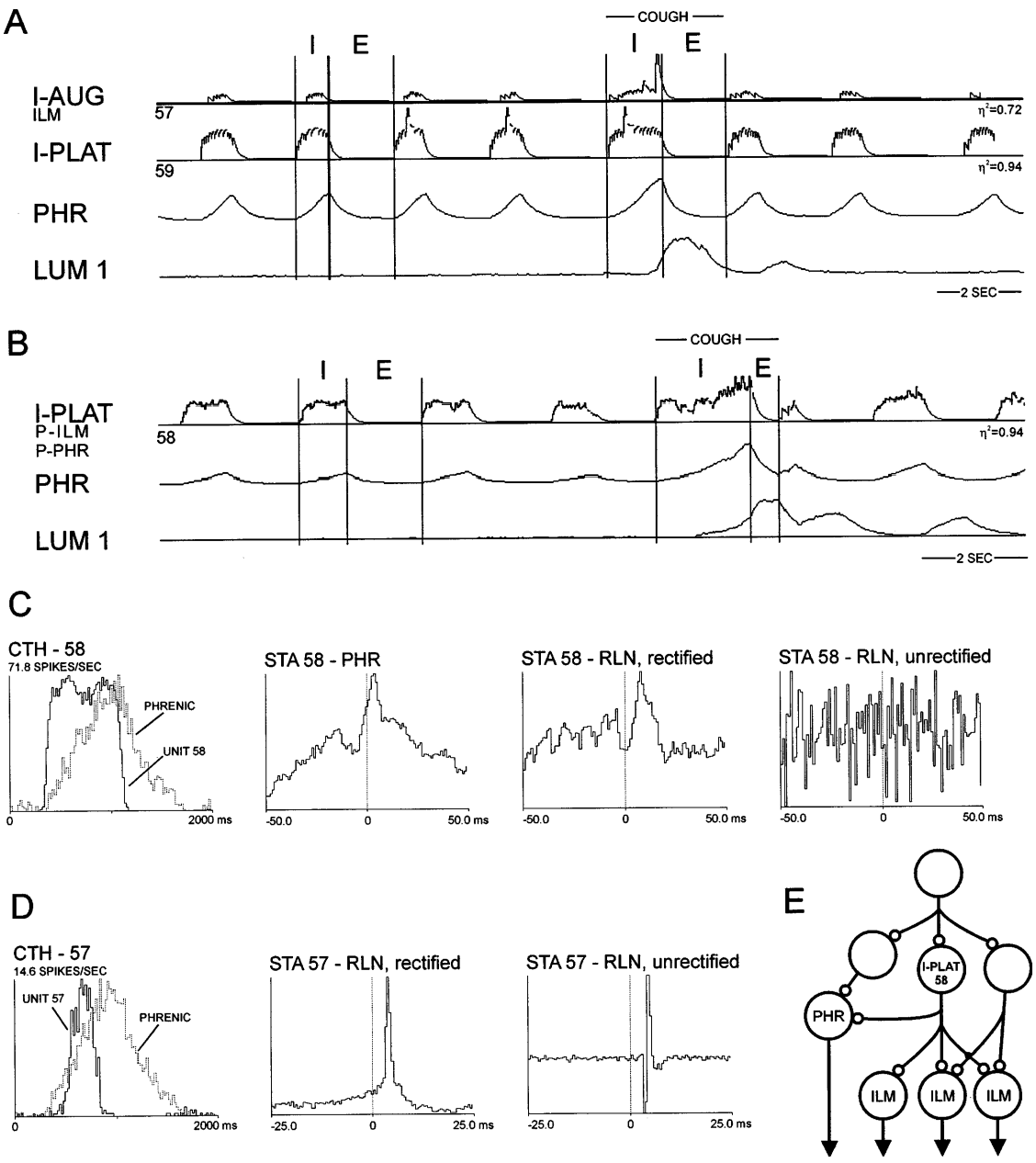

Fig. 3. *A* and *B*: putative I-DRIVER neurons in BÖT/rVRG region during fictive cough. Neuron, phrenic, and lumbar nerve discharge rates are displayed as moving time averages (100-ms time constant). η^2, Statistical measure of respiratory modulation. Unit coordinates (anteroposterior, lateral, depth) are as follows (in mm): 3.0, 4.0, 4.5 (*unit 57*); 3.6, 3.2, 4.7 (*unit 59*); 3.1, 3.9, 4.1 (*unit 58*). *C* and *D*: cycle-triggered histograms (CTH) and spike-triggered averages (STA) of putative I-DRIVER neurons. *E*: plausible interpretation of STAs in *C*. See *Glossary* for abbreviations.

expiratoryphase transition during in vivo cough (Fig. 4, *trace 2*), which supported a hypothesis for propriobulbar E-DEC neurons in the model (Fig. 2, *trace 7*). Two of these were identified with spike-triggered averaging as premotor to ELMs; the other five had negative bulbospinal and laryngeal motoneuron tests. Six other E-DEC cells showed a variety of responses during cough; three were laryngeal motoneurons.

E-AUG NEURONS (BÖT/ROSTRAL VRG). Twelve of 24 E-AUG neurons (1 BS, 0 P-PHR, 0 P-LM, 0 LM, 5 not tested) had discharge patterns similar to the lumbar nerve during in vivo cough (Fig. 5, *traces 1* and *2*). There was an earlier onset of firing, increased peak activity, and a DEC pattern. Five other E-AUG cells (0 BS, 0 P-PHR, 0 P-LM, 0 LM, 1 not tested) showed an earlier onset of discharge and an increased ramp of augmented activity during cough (Fig. 4, *traces 3* and *4*). The responses of these two groups of putative propriobulbar neurons were similar to two hypothesized subpopulations of E-AUG neurons in the model (Fig. 2, *traces 8* and *9*). The other 7 of 24 E-AUG cells (0 BS, 0 P-PHR, 1 P-LM, 0 LM, 2 not tested) decreased activity during cough (Fig. 6, *trace 1*). This attenuated response was not hypothesized or predicted by the model.

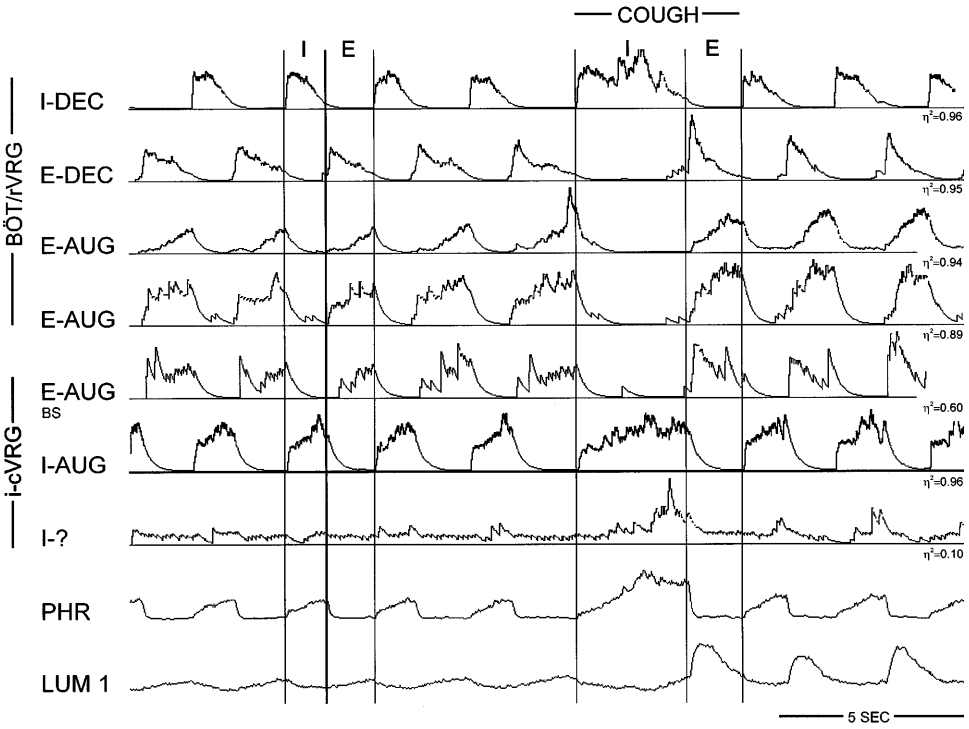

Fig. 4. Concurrent responses of BÖT/rVRG and i-cVRG neurons during fictive cough. Unit coordinates (*top* to *bottom*; anteroposterior, lateral, depth) are as follows (in mm): 3.8, 3.2, 4.3; 2.6, 3.3, 3.8; 3.0, 3.3, 3.8; 2.9, 3.4, 3.4; −1.6, 3.4, 3.9; −2.0, 3.4, 3.6; −2.0, 3.4, 3.9.

E-AUG (INTERMEDIATE-CAUDAL VRG). Eight E-AUG (BS) neurons located in the VRG, at or caudal to the obex, had discharge patterns during in vivo cough similar to the motor activity of the lumbar nerve (Fig. 4, *trace 5*). There was an earlier onset of activity beginning often during the inspiratory phase and an increase in peak activity and a DEC firing pattern during the expiratory phase. Twenty-three other E-AUG cells (0 P-LM, 1 LM) responded similarly. The responses during in vivo cough of E-AUG neurons just described agreed with the model simulations (Fig. 2, *trace 11*). One other bulbospinal and three unidentified E-AUG cells decreased peak discharge during cough.

E-RECRUIT. Fourteen neurons (11 i-cVRG, 3 BÖT/rVRG) were recruited during the expiratory phase of cough (Fig. 6, *trace 2*). Their discharge patterns were similar to the DEC pattern of the lumbar nerve. No cells had the AUG discharge pattern of the model-simulated E-RECRUIT cells (Fig. 2, *trace 10*). Two cVRG-recruited expiratory neurons were bulbospinal.

Neurons with discharge patterns not included in the simulated model. In the BÖT/rVRG region, small numbers of phase-spanning inspiratory- and expiratory-modulated neurons (n = 8 and 5, respectively) with various discharge patterns (I-EI and E-IE) during control showed even more varied responses during in vivo cough (Table 4). Neurons with low inspiratory- and expiratory-modulated firing rates (n = 17 and 10, respectively) also showed a variety of responses to cough. Nine (4 BÖT/rVRG, 5 i-cVRG) of 64 non-respiratory-modulated cells showed an increased firing rate during cough that was not associated with the inspiratory or expiratory phase but was correlated with the stimulus duration (Fig. 6, *trace 3*).

In the i-cVRG area, 11 I-DEC neurons (3 BS, 0 P-PHR, 1 P-LM, 0 LM, 3 not tested) showed an increase

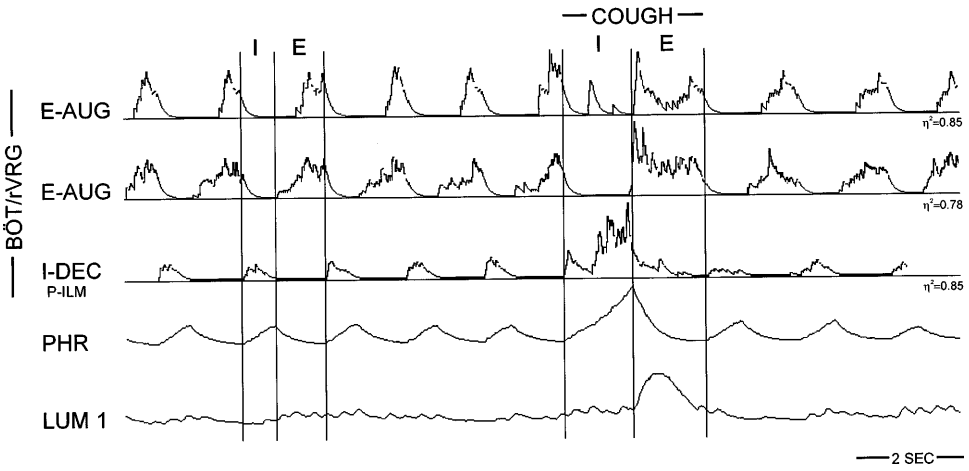

Fig. 5. Concurrent responses of BÖT/rVRG neurons during fictive cough. Unit coordinates (*top* to *bottom*; anteroposterior, lateral, depth) are as follows (in mm): 3.8, 3.4, 4.3; 4.6, 3.4, 4.5; 3.0, 3.5, 3.8.

Table 4. *Discharge patterns, axonal projections, and changes in peak firing rate of BÖT/rVRG and i-cVRG neurons during cough*

	BÖT/rVRG					i-cVRG				
			RLN					RLN		
	n	BS	PM	M	Δcg	*n*	BS	PM	M	Δcg
I-PLAT	6	0/6	1/6	1/6	2↑, 4→					
I-DEC	22	1/18	2/14	0/14	17↑, 5→	11	5/8	1/8	0/8	11↑
I-AUG	22	3/15	2/13	2/13	22↑	34	21/34	2/17	0/17	34↑
I-EI	8	1/5	0/4	0/4	6↑, 2→	5	0/4	0/4	0/4	4↑, 1→
I-IE						3	0/3	0/3	0/3	3↑
I?	17	0/7	0/10	0/10	8↑, 2↓, 7→	7	0/7	0/7	0/7	7↑
E-DEC	13	0/10	2/10	3/10	9↑, 3↓, 1→	1	0	0	0	↑
E-AUG	24	1/17	1/15	0/15	17↑, 7↓	34	8/23	0/17	1/17	30↑, 4↓
E-IE	5	0/4	0/1	0/1	3↑, 2→					
E?	10	0/8	2/6	0/6	8↑, 2↓	6	1/5	0/3	0/3	4↑, 2↓
E-RECRUIT	3	0/1	0/1	0/1	3↑	11	2/4	0/3	0/3	11↑
NRM	36				4↑, 32→	28				5↑, 23→
Total	166					140				

Number (*n*) of neurons, results of bulbospinal (BS) identification, results of spike-triggered averaging with RLN efferent activity for identification of putative motor (M) or premotoneurons (PM), and neuron peak firing rate changes during cough (Δcg: ↑, increase; ↓, decrease; →, no change) are shown. Denominator in columns BS, PM, and M represent number of cells tested. See *Glossary* for definition of other abbreviations.

in peak discharge rate during in vivo cough; nine cells changed to AUG discharge patterns, and two maintained DEC patterns during cough. Phase-spanning I-IE (n = 3) and I-EI (n = 5) exhibited a variety of discharge patterns during control and cough. Seven inspiratory cells with low firing rates during control (I?) increased activity during the inspiratory phase of cough (Fig. 4, *trace 7*). Six expiratory cells had relatively low firing rates during the control expiratory phase (E?); four increased and two decreased activity during cough.

DISCUSSION

The use of microelectrode arrays permitted the measurement of concurrent and sequential changes in discharge patterns of many neurons in the BÖT/rVRG and i-cVRG network. The cough motor pattern was associated with altered activity in all major categories of respiratory-modulated neurons as well as neurons with infrequently encountered discharge patterns. The results are consistent with many of the specific predictions derived from the network simulations and support the two principal hypotheses: *1*) bulbospinal drive to respiratory motoneurons during cough arises, at least in part, from the same medullary neurons involved in providing descending drive during normal breathing; and *2*) the BÖT/rVRG neuronal network implicated in generating and shaping the eupneic pattern of breathing is also involved in producing the cough motor pattern.

i-cVRG Bulbospinal Inspiratory and Expiratory Neuron Responses

The altered activity of bulbospinal I-AUG and E-AUG neurons during in vivo cough supports the hypothesis that they provide drive to spinal respiratory motoneurons during this reflex. Bulbospinal I-AUG neurons provide the primary drive to phrenic and inspiratory intercostal motoneurons (3, 16, 33). All I-AUG neurons, including those identified as bulbospinal, increased activity in a manner similar to phrenic motor activity during cough. All bulbospinal inspiratory neurons with decrementing discharge patterns during control periods had increased firing rates during cough, some with decrementing and some with aug-

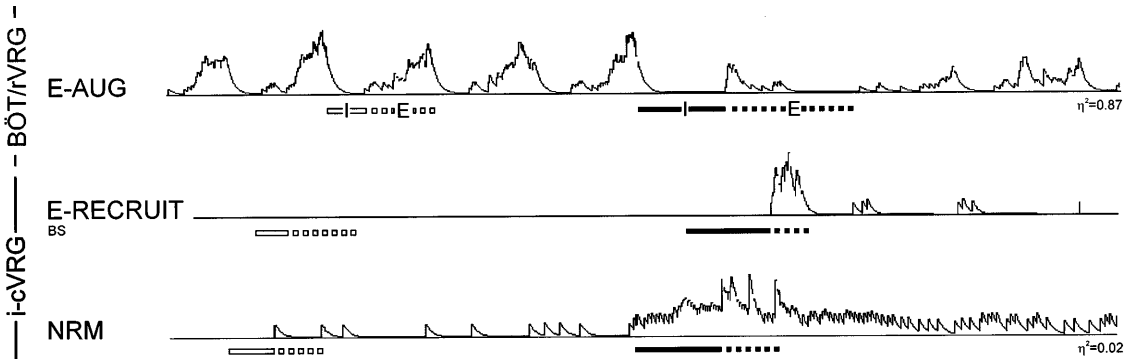

Fig. 6. Examples of BÖT/rVRG and i-cVRG expiratory neuron responses during fictive cough. Neurons are from different experimental runs and animals. Unit coordinates (*top* to *bottom*; anteroposterior, lateral, depth) are as follows (in mm): 4.6, 3.3, 3.8; −1.2, 3.4, 2.5; 1.2, 3.2, 3.7.

menting patterns. These results are supported by earlier (15, 21, 22) and recent observations (20, 37).

Bulbospinal E-AUG neurons provide drive to expiratory intercostal and abdominal motoneurons (16, 33). Most E-AUG neurons, bulbospinal as well as those with unidentified axon projections, exhibited increased activity with patterns similar to lumbar motoneuron activity during in vivo cough. Earlier studies reported increased activity of caudal ventrolateral medulla expiratory neurons during the expiratory phase of cough, but their discharge patterns and axon projections were not determined (15, 21, 22). Our results differ from those found recently by Oku et al. (37). They reported that caudal VRG bulbospinal E-AUG neuron discharge patterns during cough were not similar to abdominal motor nerve activity and proposed another source of descending drive to spinal expiratory motoneurons during cough. Our results are not inconsistent with other sources of drive contributing to the decrementing pattern of expiratory motor nerves. However, the data strongly suggest that bulbospinal E-AUG neurons are involved in shaping the pattern. The differences between the studies could be due to the type or site of stimulation used to elicit fictive cough. Mechanical stimulation of the intrathoracic trachea was employed in the present work, whereas Oku et al. used electrical stimulation of superior laryngeal nerve afferents.

Comparison of In Vivo Results and Specific Model Hypotheses on BÖT/rVRG Neurons That Produce the Cough Motor Pattern

The in vivo results support the second main hypothesis: BÖT/rVRG neurons implicated in generating the eupneic rhythm and pattern of breathing also participate in the production of the cough motor pattern. Many of the changes in discharge patterns predicted from the model simulation data were confirmed (∗ in Fig. 2); other results were not consistent with expectations.

Inspiratory phase of cough. We predicted that all categories of inspiratory neurons would be excited during in vivo cough and that their collective interactions would produce an increased ramp and duration of inspiratory premotor and motor activity. The initiation and maintenance of the eupneic inspiratory phase has been proposed to involve a subpopulation of rostral VRG inspiratory neurons that provide excitatory drive to other medullary inspiratory neurons (Figs. 1*A* and 2, *trace 1*). These neurons have been called I-Drivers (41), I-EI (2), and I-Continuous (16). We observed five rostral BÖT/rVRG neurons with I-Plateau (I-Continuous) discharge patterns that may serve such an excitatory function. On the basis of negative bulbospinal and laryngeal motoneuron tests and one positive laryngeal premotoneuron test, these neurons are classified as putative propriobulbar. The discharge patterns of these cells were similar to identified propriobulbar neurons described previously by our laboratory (34, 41) and Ezure (16). During in vivo cough the active phases of these neurons were prolonged with little or no change in peak firing rate. This result was not consistent with our original model hypothesis that cells with this function are excited by cough afferent inputs (Fig. 2, *trace 1*). Our new hypothesis is that these I-Plateau neurons influence the inspiratory phase duration and contribute a level of drive, but not changes in drive (Fig. 7, *trace 1*). This revised view is similar to that already put forward by us, for this class of cells, to account for changes in inspiratory drive and pattern caused by peripheral chemoreceptor stimulation (34).

Propriobulbar I-DEC neurons were predicted in our model to have an amplified DEC pattern during cough (Fig. 2, *trace 2*). These model cells, through inhibitory actions, help terminate the previous expiratory phase, suppress expiratory neurons during the inspiratory phase, and shape the firing profile of I-AUG cells (Fig. 1*A*). The diverse patterns of response of BÖT/rVRG I-DEC cells during in vivo cough suggested that there were at least three functional subpopulations. One group responded during cough with an amplified DEC pattern, as hypothesized and simulated. Six of these cells had negative bulbospinal and laryngeal premotoneuron and motoneuron tests; they are classified as

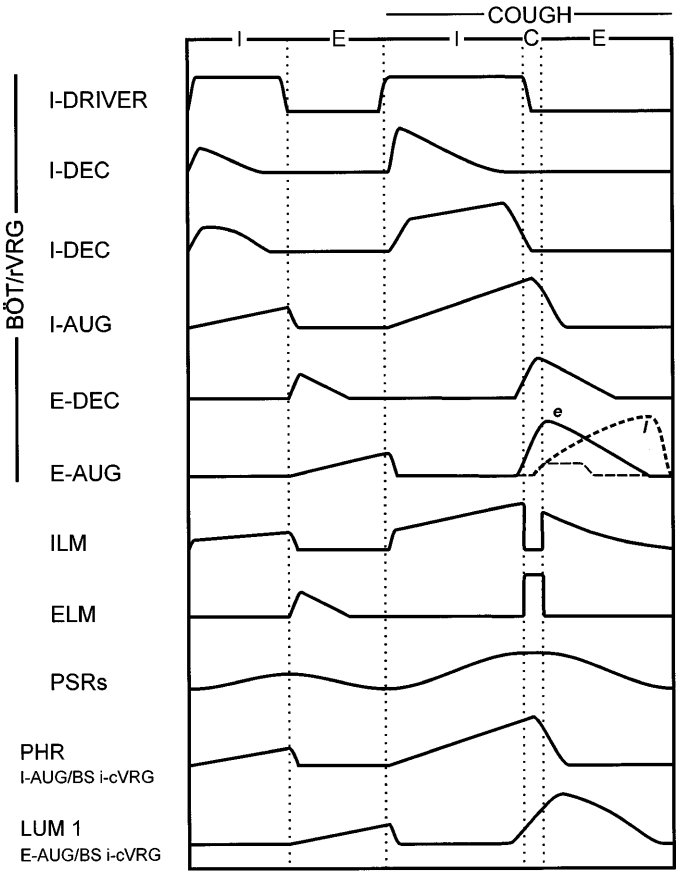

Fig. 7. Graphical representation of major classifications of observed (in vivo) respiratory neurons and their responses during fictive cough. Discharge profiles were estimated from integrated neuronal signals (in vivo). Each profile represents an envelope that includes neurons with similar discharge patterns, but different peak rates, and duration of activities. ILM and ELM discharge profiles are based on reports in literature (12, 39) and are included to place other neuron responses in full context. PSR activity is estimated and included to enhance summary.

putative propriobulbar neurons. A similar response during fictive cough was reported for identified propriobulbar I-DEC neurons during superior laryngeal nerve stimulation (37).

Five other putative propriobulbar I-DEC neurons displayed an augmenting pattern during in vivo cough. Another group of four I-DEC neurons, with brief bursts of activity in the early inspiratory phase, exhibited only an extended discharge time during cough. The responses of these two groups of neurons were not predicted or simulated by the model, and our data do not support adding them to the cough model at this time. It will be necessary to identify the functional connectivity of these specific types of cells to determine their role in eupneic and cough motor pattern generation.

As already noted, all I-AUG cells increased activity similarly to phrenic activity during in vivo cough, as proposed in the model (Fig. 2, *traces 3* and *4*). It is likely that many of the cells, particularly those in the BÖT/rVRG, were propriobulbar neurons; four were characterized as propriobulbar, i.e., premotor to ILMs. Propriobulbar I-AUG neurons drive bulbospinal I-AUG neurons, upper airway motoneurons with inspiratory modulation, and inhibit BÖT and caudal VRG E-AUG cells (3, 16, 33). Oku et al. (37) reported a similar response from identified propriobulbar I-AUG cells during fictive cough triggered by electrical stimulation of superior laryngeal nerves.

Compressive and expulsive phases of cough. Complex neuronal interactions must occur at the inspiratory-expiratory phase transition of a cough to coordinate the thoracoabdominal and upper airway muscles. The neural correlate of the compressive period was not identified in these in vivo studies, because the specific activity of laryngeal adductor motoneurons was not monitored. Therefore, the following discussion focuses on the responses and actions of other neurons during the compressive (inspiratory-expiratory phase transition) and expulsive periods.

BÖT/rVRG E-DEC and E-AUG cells play important roles, through inhibition, in terminating and suppressing the inspiratory phase and shaping the discharge patterns of caudal VRG bulbospinal E-AUG neurons and spinal expiratory motoneurons (Fig. 1*A*). During in vivo cough, seven BÖT/rVRG E-DEC neurons increased peak activity near the inspiratory-expiratory phase transition and had an extended firing duration. This response was similar to the hypothesized and simulated propriobulbar E-DEC cells (Fig. 2, *trace 7*). Evidence supporting characterization of these neurons as propriobulbar and putative propriobulbar was that two cells were premotor to laryngeal motoneurons and all had negative bulbospinal and laryngeal motoneuron tests. Oku et al. (37) reported a similar response from identified propriobulbar E-DEC cells to superior laryngeal nerve-induced fictive cough. Six other E-DEC neurons in our study responded with a variety of discharge patterns that were different from this first group; some were laryngeal motoneurons.

Two responses and several actions of BÖT/rVRG E-AUG neurons during cough were proposed in the model. E-AUG cells in the BÖT/rVRG region are primarily propriobulbar, with some having bulbospinal projections (3, 16, 23, 33). One group of neurons was predicted to switch their discharge patterns from AUG during control to DEC during cough (Fig. 2, *trace 8*); they would begin firing earlier than usual and have an increased peak firing rate. Their inhibitory action would contribute to the termination of the inspiratory phase (Fig. 1*A*). During in vivo cough the responses of most E-AUG neurons ($n = 12$) were consistent with this hypothesized first group. A second group of E-AUG neurons was postulated to begin discharging later in the phase and maintain an augmenting discharge pattern during cough; their inhibitory actions would contribute to the DEC pattern of the first subset of E-AUG neurons and caudal VRG bulbospinal expiratory neurons during cough (Fig. 1*A*). In vivo evidence was also obtained for E-AUG cells ($n = 5$) that behaved similarly to this second group during cough. Six neurons in the first group and four in this second group had negative bulbospinal and laryngeal motoneuron tests and are considered to be putative propriobulbar neurons. The activity of another smaller third group of BÖT/rVRG E-AUG neurons ($n = 7$) was attenuated during cough. These attenuated neurons may be the subpopulation, the activity of which is delayed during eupnea by the inhibitory actions of propriobulbar E-DEC neurons (2, 3, 23, 29, 30). Oku et al. (37) also reported that BÖT E-AUG cells displayed a variety of discharge patterns during cough, but they did not present specific details.

A question is raised by the present study: What network interactions are responsible for reconfiguring the discharge pattern of caudal VRG bulbospinal expiratory neurons from AUG during control to DEC during cough? One source may be excitatory inputs from the first group of observed BÖT/rVRG E-AUG cells discussed above. Their decrementing discharge patterns during in vivo cough were similar to those of caudal VRG bulbospinal expiratory neurons and the lumbar nerve. The possible contribution of these neurons was not included in the initial cough model, because available data from spike train cross-correlation data and spike-triggered averaging of synaptic potentials indicated that most functional connections among BÖT E-AUG and caudal VRG E-AUG neurons are inhibitory (23, 29). However, there were data in these two reports consistent with excitatory connections, but they were observed less frequently. There is also other, less direct, evidence that suggests that a subpopulation of BÖT E-AUG neurons may excite caudal VRG bulbospinal expiratory neurons. Electrical microstimulation and microinjection of excitatory amino acids in the BÖT region excited caudal VRG expiratory neurons (6).

The proposed cough model included a population of neurons that were silent during eupnea and recruited during cough with an augmenting discharge pattern (E-RECRUIT; Fig. 2, *trace 10*). They were a necessary addition for producing the decrementing pattern in

bulbospinal E-AUG cells. None of the recruited BÖT/rVRG and i-cVRG cells observed in vivo had the AUG discharge pattern of the simulated E-RECRUIT cells. Their pattern during cough was similar to the pattern of E-AUG neurons and the lumbar nerve. The evoked cells could be high-threshold bulbospinal or BÖT E-AUG neurons.

On the basis of these results, we revise our initial proposal for the reconfiguration of the discharge pattern of caudal VRG bulbospinal expiratory neurons from AUG during control to DEC during cough. First, the initial increased firing rate is due to excitatory inputs from PSR and cough receptors, a DEC pattern of excitation from early E-AUG neurons, and postinhibitory rebound as a consequence of reduced inspiratory neuron inhibition. Second, the subsequent decrementing firing rate is due to decreasing PSR activity, increasing inhibition from a subpopulation of propriobulbar late E-AUG neurons, and a decline in excitation from early E-AUG neurons.

Other Observed Neurons Not Included in the Original or Revised Cough Model

A variety of neuron types were not included in the original or revised cough model, primarily because of the lack of data in the literature and this study on synaptic and functional connectivity (i.e., phase-spanning I-EI, I-IE, and E-IE and low respiratory-modulated I? and E?). The unpredictable responses during cough of neurons with similar discharge patterns during control and the small numbers in each category are additional reasons these cells were not included in the revised model.

A group of I-DEC cells was recorded in the i-cVRG; some were bulbospinal. Responses during cough included accentuated DEC and AUG patterns. They were not included in the model because their bulbospinal projections are unknown. They could be exciting spinal inspiratory and/or inhibiting expiratory motoneurons. Nevertheless, they also support the hypothesis that bulbospinal drive to respiratory motoneurons during cough arises, at least in part, from the same medullary neurons involved in providing descending drive during normal breathing.

A population of continuously active, non-respiratory-modulated BÖT/rVRG and i-cVRG cells increased activity during cough in a manner that was correlated with the stimulus duration. They may be interneurons transmitting cough receptor activity to the respiratory network. These putative interneurons are not included in the revised cough model. NTS neurons in the original model were given the observed discharge profile.

Revised Cough Model

To the extent that hypotheses derived from network simulations and in vivo results fail to match, the results define gaps in knowledge and aid the design of new models and future experiments. The original cough model was based on hypotheses derived from inferred synaptic connections between neurons of the BÖT/VRG (1, 2, 4, 14, 16, 29, 34, 35, 41), responses during cough of some uncharacterized respiratory neurons (15, 21, 22), and hypothesized effects of cough receptor and PSR inputs.

The scheme in Fig. 1*B* shows revised and expanded features of a cough model that incorporates new hypotheses based on the present results and recent and overlooked reports of inferred synaptic connections (1, 3, 6, 23, 29, 34). Late-I (10, 36) and Pre-I (40) neurons, proposed to be involved in the termination of the inspiratory and expiratory phase, respectively, have not been included in the present set of revisions. Only one Late-I cell had the discharge characteristics described by Cohen et al. (10), with the onset of activity delayed during an extended inspiratory phase. Although a few cells with Pre-I discharge patterns were recorded and their changes in activity during cough were consistent with their proposed function, they are not included in the revised model because of the lack of spike correlation data to support proposed synaptic connections in adult animals.

Summary of model revisions. 1) Hypothesized excitatory connections from NTS second-order cells to I-DRIVER neurons have been deleted. Putative I-DRIVER cells showed little or no change in peak firing rate during in vivo cough, suggesting that they are not excited by cough afferent input.

2) Excitatory connections from NTS second-order cells to I-DEC neurons have been added. Most I-DEC neurons increased peak firing rate during in vivo cough; this excitation is proposed to be due in part to cough afferent input.

3) E-RECRUIT neurons have been deleted. There was no in vivo evidence for E-RECRUIT neurons with augmenting discharge patterns.

4) Inhibitory connections from propriobulbar I-AUG to propriobulbar (BÖT) and bulbospinal (cVRG) E-AUG neurons have been added on the basis of data from spike-triggered averaging and cross-correlation studies (1, 3, 34, 35).

5) Inhibitory connections from E-DEC to I-DEC neurons have been added on the basis of inferences from the comparison of membrane potential trajectories (3, 14).

6) Excitatory connections from E-AUG (early) to E-AUG (BS) cells have been added on the basis of spike-triggered averaging, cross-correlation, and electrical and chemical stimulation data (6, 23, 29). Most BÖT/rVRG E-AUG cells observed in vivo had discharge patterns similar to caudal VRG bulbospinal E-AUG cells, which is consistent with the proposed excitatory connections.

7) A new subpopulation of E-AUG neurons will be added. Some BOT/rVRG E-AUG cells discharging primarily in the latter part of the eupneic expiratory phase decreased activity during in vivo cough. They are proposed to have functional connections similar to the other late E-AUG population; i.e., they inhibit E-DEC, early E-AUG, and E-AUG (BS) neurons and are inhibited by E-DEC and early E-AUG cells. It is further proposed that they do not receive excitatory inputs

from NTS second-order cough neurons or PUMP cells. It is hypothesized that, during cough, increased activity in E-DEC and early E-AUG neurons inhibit these E-AUG cells, which in turn leads to disinhibition of their target neurons.

Future simulations will determine whether these model revisions are sufficient to generate neuronal discharge patterns found in vivo. In addition to producing those patterns already confirmed, the goal is to generate a model in which a subpopulation of propriobulbar E-AUG cells decreases activity during cough.

Summary of specific hypotheses in revised model. Figure 7 is a graphical representation of the major classifications of observed respiratory neurons and their responses during fictive cough, along with phrenic and lumbar nerve and PSR activities. ILM and ELM discharge profiles are based on reports in the literature (12, 39) and are included to place the other neuron responses in full context.

INSPIRATORY PHASE OF COUGH. Cough afferents excite second-order NTS neurons, which, in turn, excite (directly or indirectly) propriobulbar I-AUG and I-DEC and premotor bulbospinal inspiratory [I-AUG (BS)] neurons. This action leads to an increased ramp and duration of inspiratory motor activity. ILM activity is also increased. Expiratory neurons are suppressed by inhibitory actions of propriobulbar I-DEC and I-AUG neurons. The duration of the inspiratory phase is determined in part by I-DRIVER neurons. Inspiration is terminated by the inhibitory actions of propriobulbar E-DEC and early E-AUG cells. The increased E-DEC and E-AUG neuron activity is due in part to reduced inhibitory actions of I-AUG and I-DEC neurons and excitation from increased PSR and cough receptor activity.

COMPRESSIVE PHASE OF COUGH. A large increase in the firing rate of bulbospinal premotor expiratory neurons [E-AUG (BS)] occurs near the end of the inspiratory phase primarily because of excitation by cough receptors and PSRs. Other factors that promote this expiratory activity include reduced inhibition from propriobulbar I-DEC and I-AUG neurons, the resulting postinhibitory rebound, and reduced inhibition and increased excitation by different subpopulations of propriobulbar E-AUG neurons. At the end of the compressive phase, ELM activity, which increased concurrently with the premotor expiratory neurons, ceases.

EXPULSIVE PHASE OF COUGH. For a short time after the compressive phase the firing rates of E-AUG (BS) neurons, and thus E motoneurons (EXP MN), continue to increase. As the expiratory phase progresses further, discharge rates decrease in a decrementing pattern shaped by decreasing PSR activity and a decline in excitation from propriobulbar early E-AUG neurons and increasing inhibition from other propriobulbar late E-AUG neurons. ILM activity is elevated again during this phase.

Summary

The present work provides evidence for the involvement of the ventrolateral medullary respiratory network in the configuration of the cough motor pattern. It is the first report of simultaneous recordings of many single neurons during cough. The observations documented changes in discharge patterns of multiple neurons under identical conditions. The results supported many of our cough model predictions for specific categories of neurons (i.e., bulbospinal I-AUG and E-AUG and propriobulbar I-DEC, I-AUG, E-DEC, and E-AUG). I-DRIVER and E-RECRUIT cells did not respond as expected. A revised cough model is presented. Other categories of neurons were observed, but the results did not support their inclusion in the model (i.e., phase-spanning I-EI, I-IE, and E-IE; low respiratory-modulated I? and E?; excited NRM; i-cVRG bulbospinal I-DEC).

We gratefully acknowledge the technical support of Jan Gilliland, Rebecca McGowan, Zhongzeng Li, and Peter Barnhill.

This study was supported by National Heart, Lung, and Blood Institute Grant HL-49813.

Preliminary accounts of these results have been published (42, 43).

Address for reprint requests: R. Shannon, Physiology and Biophysics, MDC Box 8, College of Medicine, University of South Florida, Tampa, FL 33612.

Received 20 February 1997; accepted in final form 3 February 1998.

REFERENCES

1. **Anders, K., D. Ballantyne, A. M. Bischoff, P. M. Lalley, and D. W. Richter.** Inhibition of caudal medullary expiratory neurones by retrofacial inspiratory neurones in the cat. *J. Physiol. (Lond.)* 437: 1–25, 1991.
2. **Balis, U. J., K. F. Morris, J. Koleski, and B. G. Lindsey.** Simulation of ventrolateral medullary neural network for respiratory rhythmogenesis inferred from spike train cross-correlation. *Biol. Cybern*. 70: 311–327, 1994.
3. **Bianchi, A. L., M. Denavit-Saubie, and J. Champagnat.** Central control of breathing in mammals: neuronal circuitry, membrane properties, and neurotransmitters. *Physiol. Rev*. 75: 1–45, 1995.
4. **Bianchi, A. L., L. Grelot, S. Iscoe, and J. E. Remmers.** Electrophysiological properties of rostral medullary respiratory neurones in the cat: an intracellular study. *J. Physiol. (Lond.)* 407: 293–310, 1988.
5. **Bolser, D. C.** Fictive cough in the cat. *J. Appl. Physiol*. 71: 2325–2331, 1991.
6. **Bongianni, F., M. Corda, G. Fontana, and T. Pantaleo.** Expiration-related neurons in the caudal ventral respiratory group of the cat: influences of the activation of Bötzinger complex neurons. *Brain Res*. 526: 299–302, 1990.
7. **Botteron, G. W., and P. D. Cheney.** Corticomotoneronal postspike effects in averages of unrectified EMG activity. *J. Neurophysiol*. 52: 1127–1139, 1989.
8. **Christakos, C. N., M. I. Cohen, R. Barnhardt, and C. F. Shaw.** Fast rhythms in phrenic motoneuron and nerve discharges. *J. Neurophysiol*. 66: 674–687, 1991.
9. **Christakos, C. N., M. I. Cohen, A. L. Sica, W. Huang, W. R. See, and R. Barnhardt.** Analysis of recurrent laryngeal inspiratory discharges in relation to fast rhythms. *J. Neurophysiol*. 72: 1304–1316, 1994.
10. **Cohen, M. I., W. Huang, R. Barnhardt, and W. R. See.** Timing of medullary late-inspiratory neuron discharges: vagal afferent effects indicate possible off-switch function. *J. Neurophysiol*. 69: 1784–1787, 1993.
11. **Connelly, C. A., E. G. Dobbins, and J. L. Feldman.** Pre-Bötzinger complex in cats: respiratory neuronal discharge patterns. *Brain Res*. 590: 337–340, 1992.
12. **Dawid-Milner, M. S., J. P. Lara, A. Milan, and S. Gonzalez-Baron.** Activity of inspiratory neurones of the ambiguus complex during cough in the spontaneously breathing decerebrate cat. *Exp. Physiol*. 78: 835–838, 1993.

13. **Duffin, J., and D. Aweida.** The propriobulbar respiratory neurons in the cat. *Exp. Brain Res.* 81: 213–220, 1990.
14. **Duffin, J., K. Ezure, and J. Lipski.** Breathing rhythm generation: focus on the rostral ventrolateral medulla. *News Physiol. Sci.* 10: 133–140, 1995.
15. **Engelhorn, R., and E. Weller.** Zentrale representation hustenwirksamer afferenzen in der medulla oblongata der katze. *Pflügers Arch.* 284: 224–239, 1965.
16. **Ezure, K.** Synaptic connections between medullary respiratory neurons and considerations on the genesis of respiratory rhythm. *Prog. Neurobiol.* 35: 429–450, 1990.
17. **Ezure, K., K. Otake, J. Lipski, and R. B. Wong She.** Efferent projections of pulmonary rapidly adapting receptor relay neurons in the cat. *Brain Res.* 564: 268–278, 1991.
18. **Feldman, J. L., and H. H. Ellenberger.** Central coordination of respiratory and cardiovascular control in mammals. *Annu. Rev. Physiol.* 50: 593–606, 1988.
19. **Feldman, J. L., and J. C. Smith.** Neural control of respiratory pattern in mammals: an overview. In: *Regulation of Breathing*, edited by T. F. Hornbein. New York: Dekker, 1995, vol. 79, p. 39–69. (Lung Biol. Health Dis. Ser.)
20. **Gestreau, C., S. Milano, A. L. Bianchi, and L. Grelot.** Activity of dorsal respiratory group inspiratory neurons during laryngeal-induced fictive coughing and swallowing in decerebrate cats. *Exp. Brain Res.* 108: 247–256, 1996.
21. **Jakus, J., Z. Tomori, and A. Stransky.** Activity of bulbar respiratory neurons during cough and other respiratory tract reflexes in cats. *Physiol. Bohemoslov.* 34: 127–136, 1985.
22. **Jakus, J., Z. Tomori, A. Stransky, and L. Boselova.** Bulbar respiratory activity during defensive airways reflexes in cats. *Acta Physiol. Hung.* 70: 245–254, 1987.
23. **Jiang, C., and J. Lipski.** Extensive monosynaptic inhibition of ventral respiratory group neurons by augmenting neurons in the Bötzinger complex in the cat. *Exp. Brain Res.* 81: 639–648, 1990.
24. **Kirkwood, P. A., and T. A. Sears.** Cross-correlation analyses of motoneuron inputs in a coordinated motor act. In: *Neuronal Cooperativity*. Berlin: Springer-Verlag, 1991, p. 225–248.
25. **Korpas, J., and Z. Tomori.** Cough and other respiratory reflexes. *Prog. Respir. Res.* 12: 190–217, 1979.
26. **Korten, J. B., and G. G. Haddad.** Respiratory waveform pattern recognition using digital techniques. *Comput. Biol. Med.* 19: 207–217, 1989.
27. **Kubin, L., and R. O. Davies.** Central pathways of pulmonary and airway vagal afferents. In: *Regulation of Breathing*, edited by T. F. Hornbein. New York: Dekker, 1995, vol. 79, p. 219–284. (Lung Biol. Health Dis. Ser.)
28. **Lindsey, B. G., Y. M. Hernandez, K. F. Morris, R. Shannon, and G. L. Gerstein.** Dynamic reconfiguration of brainstem neural assemblies: respiratory phase-dependent synchrony vs. modulation of firing rates. *J. Neurophysiol.* 67: 923–930, 1992.
29. **Lindsey, B. G., L. S. Segers, and R. Shannon.** Functional associations among simultaneously monitored lateral medullary respiratory neurons in the cat. II. Evidence for inhibitory actions of expiratory neurons. *J. Neurophysiol.* 57: 1101–1117, 1987.
30. **Lindsey, B. G., L. S. Segers, and R. Shannon.** Discharge pattern of augmenting expiratory neurons in rostral lateral medulla of cat: regulation by concurrent network processes. *J. Neurophysiol.* 61: 1185–1196, 1989.
31. **MacGregor, R. J.** *Neural and Brain Modeling.* New York: Academic, 1987, p. 1–643.
32. **Montano, N., T. Gnecchi-Ruscone, A. Porta, F. Oombardi, A. Malliani, and S. M. Barman.** Presence of vasomotor and respiratory rhythms in the discharge of single medullary neurons involved in the regulation of cardiovascular system. *J. Auton. Nerv. Syst.* 57: 116–122, 1996.
33. **Monteau, R., and G. Hilaire.** Spinal respiratory motoneurons. *Prog. Neurobiol.* 37: 83–144, 1991.
34. **Morris, K. F., A. Arata, R. Shannon, and B. G. Lindsey.** Inspiratory drive and phase duration during carotid chemoreceptor stimulation: medullary neurone correlations. *J. Physiol. (Lond.)* 491: 241–259, 1996.
35. **Ogilvie, M. D., A. Gottschalk, K. Anders, D. W. Richter, and A. I. Pack.** A network model of respiratory rhythmogenesis. *Am. J. Physiol.* 263 (*Regulatory Integrative Comp. Physiol.* 32): R962–R975, 1992.
36. **Oku, Y., I. Tanaka, and K. Ezure.** Possible inspiratory off-switch neurones in the ventrolateral medulla of the cat. *Neuroreport* 3: 933–936, 1992.
37. **Oku, Y., I. Tanaka, and K. Ezure.** Activity of bulbar respiratory neurons during fictive coughing and swallowing in the decerebrate cat. *J. Physiol. (Lond.)* 480: 309–324, 1994.
38. **Orem, J., and T. Dick.** Consistency and signal strength of respiratory neuron activity. *J. Neurophysiol.* 50: 1098–1107, 1983.
39. **Sant'Ambrogio, G.** Coughing: an airway defensive reflex. In: *Pathophysiology of the Gut and Airways. Studies in Physiology I.* Chapel Hill, NC: Portland, 1993, p. 89–96.
40. **Schwarzacher, S. W., J. C. Smit, and D. W. Richter.** Pre-Bötzinger complex in the cat. *J. Neurophysiol.* 73: 1452–1461, 1995.
41. **Segers, L. S., R. Shannon, S. Saporta, and B. G. Lindsey.** Functional associations among simultaneously monitored lateral medullary respiratory neurons in the cat. I. Evidence for excitatory and inhibitory actions of inspiratory neurons. *J. Neurophysiol.* 57: 1078–1100, 1987.
42. **Shannon, R., D. M. Baekey, K. F. Morris, and B. G. Lindsey.** Brainstem respiratory networks and cough. *Pulm. Pharmacol.* 9: 343–347, 1997.
43. **Shannon, R., D. C. Bolser, and B. G. Lindsey.** Neural control of coughing and sneezing. In: *Neural Control of the Respiratory Muscles*. Boca Raton, FL: CRC, 1996, p. 213–222.
44. **Widdicombe, J. G.** Reflexes from the upper respiratory tract. In: *Handbook of Physiology. The Respiratory System. Control of Breathing*. Bethesda, MD: Am. Physiol. Soc., 1986, sect. 3, vol. II, pt. 1, chapt. 11, p. 363–394.
45. **Widdicombe, J. G.** Neurophysiology of the cough reflex. *Eur. Respir. J.* 8: 1193–1202, 1995.